Olmeda, P.; Margot, X.; Quintero-Igeño, P.; Escalona-Cornejo, JE. (2020). Numerical approach to define a thermodynamically equivalent material for the conjugate heat transfer simulation of very thin coating layers. International Journal of Heat and Mass Transfer. 162:1-9. https://doi.org/10.1016/j.ijheatmasstransfer.2020.120377

Numerical approach to define a thermodynamically equivalent material for the Conjugate Heat Transfer simulation of very thin coating layers

P. Olmeda, X. Margot*, P. Quintero, J. Escalona

CMT – Motores Térmicos, Universitat Politècnica de València, Camino de Vera, 46022 Valencia, Spain

Abstract

The 3D Conjugate Heat transfer (CHT) calculation of the heat transfer from the gas to the walls of a combustion chamber requires very fine meshing, particularly so when the walls are coated with a very thin insulation layer. It is practically impossible to mesh such thin layers for numerical as well as computational cost reasons. In this paper a solution to this problem is presented: an equivalent material layer with a reasonable meshing thickness is defined in such a way that its thermal behavior matches that of the real very thin coating layer. The methodology used to define the thermodynamic properties of the equivalent coating material is based on a combination of a 1D heat transfer model and a multi-factorial sweep of material properties. This equivalent material layer can then be introduced in the 3D CHT calculation instead of the real coating thin layer, and can be adequately meshed to predict with accuracy the heat losses. The approach is illustrated for a real case and a parametric study is performed to evaluate the importance of the number of mesh nodes and the material thickness.

Keywords: Temperature swing, Coating material, ICE, Conjugate Heat Transfer, 1D heat transfer model

1. Introduction

For many decades now, automobile manufacturers have worked towards achieving higher Internal Combustion Engine (ICE) efficiency, and this has become even more important now in view of environmental issues and severe emissions restrictions [1]. More recently, efforts are directed at reducing heat transfer losses because they represents an important percentage of about 35-40% of the total losses in an ICE [2]. This is even more important in small engines destined for hybrid vehicle solutions.

In pursuit of this objective there appeared in the early 1980s the concept of Low Heat Rejection (LHR) engines that consisted in manufacturing the combustion chamber walls of Diesel engines with a ceramic material of low thermal conductivity and high heat capacitance [3]. The idea was to reduce the thermal gradient between the in-cylinder gas and the combustion chamber walls. This is an extended application of thermal barrier coatings (TBC) applied in gas turbines [4], where innovative materials are used to achieve higher operational temperatures and fabricated to resist extreme conditions [5].

This kind of design for automotive engines was studied in several investigations [6–8] and these concluded that it presented serious disadvantages in terms of engine performance, which made its application difficult. The main problem of this concept is the high temperature on the surface of the combustion chamber walls, which causes the deterioration of the combustion process, thus affecting the fuel consumption and producing exhaust gas emissions with inadequate levels of pollutants substances, such as NOx in Diesel engines [9–11]. In gasoline engines the high temperatures of the wall surfaces can also induce the occurrence of knocking [2, 12, 13]. As demonstrated by [14], the use of materials with a good resistance for high temperatures is not enough to get an improvement of the ICE thermal efficiency. However the TBC has had an extended use for improving the resistance of the engines to thermal stresses and increasing the durability of the components.

In order to reduce ICE heat losses it would be necessary to decrease the heat transfer coefficient and the thermal gradient between the in-cylinder gas and the combustion chamber walls [9]. The heat transfer coefficient, however, cannot be modified because it depends on the operational point and on the gas properties. The thermal gradient, on the other hand, can be minimized if the wall temperature follows that of the gas as closely as possible. The so-called temperature swing between gas and walls can only be obtained by applying a special insulating material on the chamber walls.

Some studies carried out by applying a thin coating of low thermal conductivity and low heat capacitance on the combustion chamber walls showed that a material with these properties could help improve the thermal efficiency of ICEs [15]. Indeed, this type of insulation promotes that the walls follow instantaneously the in-cylinder gas

*Corresponding author. Tel.: +34 963 877 650,
Email address: pabolgon@mot.upv.es (P. Olmeda), xmargot@mot.upv.es (X. Margot), pedquiig@mot.upv.es (P. Quintero), joescor2@mot.upv.es (J. Escalona)

temperature, which implies the reduction of the thermal gradient between the gas and the walls. The concept of Thermal Swing Wall Insulation was first introduced by Kosaka et al. [9] in 2013 to designate this type of coating. Kikusato et al [2] carried out numerical studies about the application of these coatings on the combustion chamber walls. They observed an improvement of the thermal efficiency for a material with very low thermal conductivity and heat capacitance. In 2016 Toyota [16] introduced on the market a turbocharged Diesel engine with a piston bowl coated with a material denominated SiRPA (silica reinforced porous anodized aluminum) and claimed significant improvements of the engine thermal efficiency. All the studies mentioned above proved that the coating layer should have low thermal conductivity and low thermal capacitance, as well as an optimal thickness. This is important to avoid the deterioration of the intake air heating [2, 16–18] and reduce effectively the thermal losses.

Experimental tests to evaluate the thermo swing behavior of the coatings in combustion engines is a most challenging problem due to the difficulty of setting sensors on the combustion chamber walls to measure the instantaneous surface temperature. Some alternative measurement techniques, such as the Laser induced phosphorescence thermometry [19] have been developed, which try to capture the thermal swing. However, they require complex special equipment and are not fully reliable.

On the other hand, from the numerical point of view, simple 1D models can be used to describe the thermal behavior of the coating materials [2, 20, 21]. But they cannot yield detailed information about the wall temperature distribution for instance. Yet, in the case of gasoline engines it is especially interesting to determine the wall temperature distribution on the combustion chamber surfaces, in order to identify possible hot spots. These are known to induce knocking phenomenon affecting the engine performance.

Though there are many studies about the application of TBC in ICE, few of them deal with Computational Fluid Dynamics (CFD) studies of ICE with coated combustion chamber walls [22–24]. To our knowledge there are no CFD studies about the new kind of thermal coatings mentioned above. This is probably due to the difficulties linked mainly to the computational cost involved in coupling the calculation of the gas flow with that of the heat transfer through the walls, the so-called Conjugate Heat Transfer (CHT) method [25–28].

The 3D-CHT calculation of the heat transfer from the gas to the walls of a combustion chamber becomes even prohibitive when the walls are thermally insulated with a very thin coating layer (of the order of 100 μm), as is the case for the recent studies mentioned above. Indeed, it is practically impossible to mesh such thin layers for numerical as well as cost reasons. This limitation could be overcome by defining an equivalent insulating layer of viable thickness (meaning a thickness that could be meshed) that would behave like the real coating layer.

In this paper a methodology is presented whereby a 1D heat transfer model is used in combination with multifactorial tests to define the thermodynamic properties (conductivity and heat capacitance) of an equivalent coating material with reasonable thickness (e.g. 2 mm). The equivalent ‘ thick” insulating layer obtained behaves as the real very thin coating layer in terms of heat fluxes and wall temperature evolution. The final goal (out of this paper's scope) is to use the equivalent material layer in 3D-CHT calculations with a thickness that can be adequately meshed, thus allowing the accurate prediction of the engine heat losses.

This paper is structured as follows: In section 2 the one dimensional heat transfer model (1D HTM) used to calculate the thermal properties of the coating materials is described in detail. Section 3 presents the methodology followed to define the equivalent coating material that will allow replacing the real very thin layer of insulating material in the CHT calculations. The methodology is demonstrated in section 4, where the results are discussed and an additional parametric study performed. Finally, the conclusions of this study are summarized in section 5.

2. 1D Numerical model

The 1D numerical lumped model [29] employed in this work is based on a previously validated heat transfer model [30]. However, coating layers were not considered. The program was accordingly modified to enable the calculation of the thermal swing expected from the insulating material. The ability of the program's new version to reproduce the thermal behavior of the insulation coatings has been verified by comparison with the analytic solution proposed by [31] and presented below.

To calculate the instantaneous heat transfer through an engine coated solid surface the following boundary conditions have to be taken into account:

For the fluid:

- On one side of the solid (in cylinder combustion chamber), both the heat transfer coefficient (h) and the gas temperature (T_g) vary with time during a thermodynamic cycle.
- On the other side (coolant side), both the heat transfer from gas to walls and the coolant temperature can be assumed to be constant with time during a thermodynamic cycle.

For the solid:

- On the side in contact with the hot gas, the conductivity, density, specific heat and thickness of the insulating material have to be imposed.
- On the coolant side the conductivity, density, specific heat and thickness of the metal are given.

There is no verifiable solution to this problem. So the first step is to validate the modified 1D-HTM. For this the simple theoretical case of a semi-infinite solid [31] is chosen, since it is possible to calculate its analytic solution. It is depicted in the scheme of Fig. 1. The following hypotheses were assumed:

- Semi-infinite solid

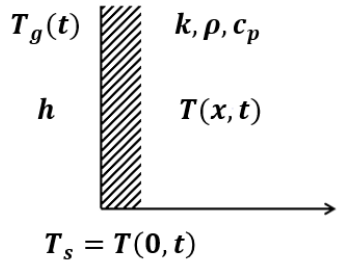

Figure 1: Scheme of the semi-infinite solid

- Constant heat transfer coefficient h between the gas and the solid surface
- Gas temperature variation according to:

$$T_g(t) = T_{gm} + \Delta T_g \cos(\omega t) \tag{1}$$

where t is the time, T_{gm} is the average gas temperature, ΔT_g is the amplitude of gas temperature and ω is the gas temperature period.

$$\omega = 2\pi n f_0 \tag{2}$$

where n represents the harmonic number and f_0 is the fundamental frequency.

- Boundary condition at solid surface:

$$\dot{q} = h(T_g - T_s) = -k\frac{\partial T}{\partial y}\bigg|_{x=0} \tag{3}$$

where T_s represents the solid temperature at the surface and T represents the solid temperature at any point of the solid.

In this case the unsteady one dimensional heat conduction equation has to be solved in the semi-infinite solid:

$$\frac{\partial T(x,t)}{\partial t} = \alpha \frac{\partial^2 T(x,t)}{\partial x^2} \tag{4}$$

where α represents the thermal diffusivity:

$$\alpha = \frac{k}{\rho c_p} \tag{5}$$

and k, ρ and c_p are the conductivity, density and specific heat of the material, respectively.

The solution for the solid temperature with the proposed boundary condition is:

$$T(x,t) = T_{gm} + \Delta T_g \cdot A \cdot e^{-\bar{x}} \cdot \cos(\omega t - \beta) \tag{6}$$

and rearranging the terms in the equation:

$$\frac{T(x,t) - T_{gm}}{\Delta T_g} = A \cdot e^{-\bar{x}} \cdot \cos(\omega t - \beta) \tag{7}$$

where A and β are respectively the amplitude and the phase shift of the surface temperature.

The amplitude A is given by:

$$A = \frac{Bi}{(Bi^2 + 2Bi + 2)^2} \tag{8}$$

where Bi is the Biot number:

$$Bi = \frac{h}{k}\sqrt{\frac{\alpha}{\pi n f_0}} \tag{9}$$

The value of the instantaneous temperature at the solid surface holds for x=0

$$\bar{x} = \sqrt{\frac{\pi n f_0}{\alpha}} x \tag{10}$$

$$\beta = -\sqrt{\frac{\pi n f_0}{\alpha}} x - tan^{-1}\frac{1}{1+Bi} \tag{11}$$

$$\frac{T(0,t) - T_{gm}}{\Delta T_g} = \frac{Bi}{(Bi^2 + 2Bi + 2)^2} \cdot \cos(\omega t - tan^{-1}\frac{1}{1+Bi}) \tag{12}$$

As seen above, the amplitude of the surface temperature and the phase shift depend on the Biot number, which can be rewritten as:

$$Bi = \frac{h}{\sqrt{k\rho c_p \pi n f_0}} \tag{13}$$

Fig. 2 presents the comparison of the analytic solution presented above and the modified 1D-HTM lumped model solution. The good agreement between both temperatures confirms the reliability of the numerical model for predicting the evolution of the coated surface temperature. It can therefore be used with confidence to solve the coated engine heat transfer problem.

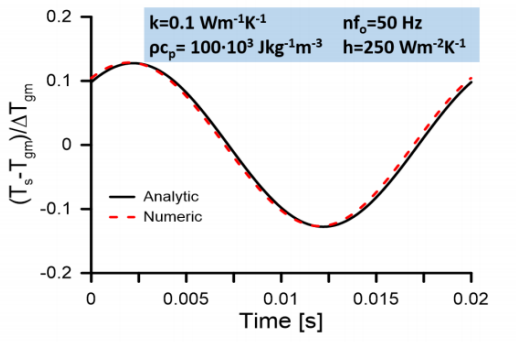

Figure 2: Surface temperature evolution calculated with numerical model and analytic solution with same boundary conditions

3. Methodology

Reducing heat losses in engines has become a crucial issue to improve engine thermal efficiency, especially in downsized engines used in electrified vehicles. One of the solutions that has been proposed by car manufacturers [9, 17] is the use of insulating materials to coat different parts of the engine, such as the piston or the cylinder head. However, it is important to assess the real impact of the coating on heat losses and engine thermal efficiency. Numerical models available in the literature and measurement techniques have some limitations and are not always reliable. For instance, 1D thermodynamic models are generally used with satisfactory results. However, they do not take into account secondary heat fluxes in other than the preferential direction, so that some inaccuracies may arise.

For a better prediction of the heat transfer through the walls, Conjugate Heat Transfer simulations may be more appropriate, especially for deepening the understanding of the heat losses mechanism. Indeed, CHT can provide secondary information, such as the time dependent temperature distribution on the solid, the distribution of the heat transfer through the different walls, and the impact of the coating on the combustion process. However, due to the thinness of the coating material layers that are commonly used [2, 9, 17], extremely fine meshing is required for the coated walls, to the point that it becomes impossible to implement. This work presents a methodology that provides a solution to the latter problem by using a 1D-HTM model. It is used to define the properties of an equivalent coating material that can then be used in the CHT simulations without the need for too fine meshes.

3.1. Calculation of equivalent coating

The proposed approach is summarized in Figure 3. On the one hand, the heat transfer coefficient (h) and the near-wall temperature of the gas (T_g) coming from a 0D-1D combustion model or from experimental data are used as boundary conditions for the calculation with the 1D heat transfer model that incorporates the real coating with its different layers. The model takes into account the characteristics of the different layers that form the real coating, including the thickness. This calculation yields the temperature wall evolution during an engine cycle (T_w) and the instantaneous heat flux at the surface. On the other hand, for the CHT calculation it is necessary to define a one layer coating with a thickness allowing reasonable meshing, and whose behavior should be equivalent to the real one. Hence, using the same boundary conditions as for the 1D model, and setting as additional input a defined thickness for the equivalent coating, a multi-factorial DoE (Design of Experiments) test is carried out. This is based on different combinations of heat capacitance and conductivity for the equivalent coating material to be defined. The instantaneous heat flux and the wall temperature swing of the 'equivalent material' obtained with the test are compared with the values obtained for the real coating. Then a multiple regression analysis is applied to the multifactorial test data to obtain a sweep of properties combinations. Finally, the equivalent coating material is chosen based on two criteria: it should be the one with the lowest error in positive and negative heat fluxes, and its thermal swing must have a very similar behavior to that of the real coating. The positive heat flux is defined as that from the gas to the wall. This 'equivalent material' with an acceptable thickness will be used to perform 3D-CHT simulations, replacing the real coating and allowing for very substantial computing savings.

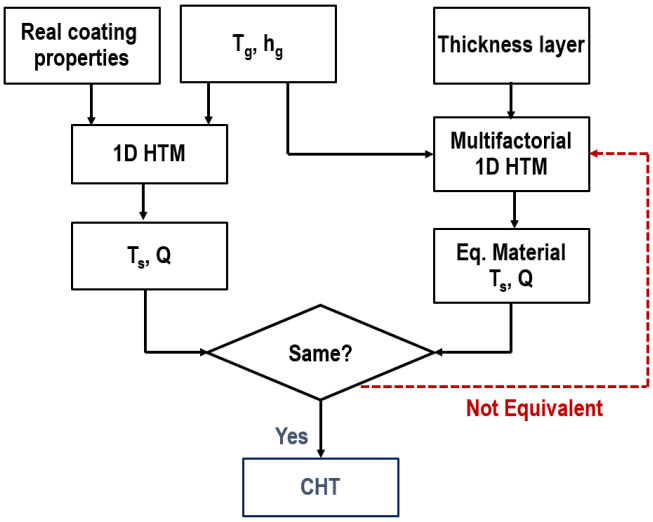

Figure 3: Equivalent material scheme methodology

3.2. Approach justification

As explained above, since coating layers for ICE walls tend to be very thin (around 100 μm), the mesh needed to calculate the heat transfer through the coated surfaces using CHT has to be extremely fine to achieve good accuracy. This increases drastically the total number of cells, and the computational cost. Fig. 4 shows the mesh for two different coating thicknesses.

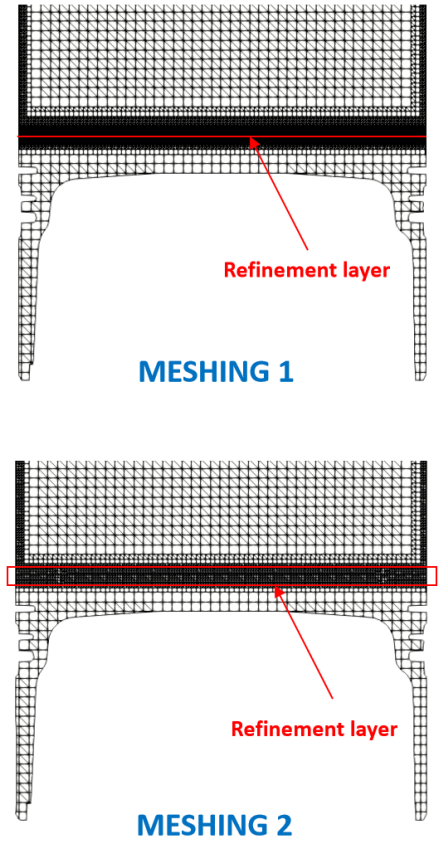

Figure 4: CHT mesh for 100 μm coating layer (top) and for 2 mm coating layer (bottom)

The coating on the piston surface in mesh 1 has a thickness of 100 μm. As seen on the figure, a very fine mesh is needed to model properly the boundary layer near the wall and the wall itself. Modeling this coating would yield a mesh with 50 million cells approximately, which is quite impossible from the computational point of view. Fig. 4 bottom shows the mesh for a 2 mm coating layer of 'equivalent material' on the piston wall. In this case the total number of cells is reduced to about 1.5 million cells, which may be used for the CHT calculation at a reasonable computational cost. This motivates the definition and subsequent use in CFD-CHT of an 'equivalent' coating layer.

4. Results and discussions

4.1. Multifactorial test

The methodology described above is illustrated for a Diesel engine operating at 1500 rpm and 14 bar. First, the heat flux and the temperature of the gas exposed wall are calculated with the 1D-HTM model. The boundary conditions, i.e. the heat transfer coefficient and the gas in-cylinder temperature of this operating condition have been previously calculated by a 0D combustion model based on experimental measurements [32, 33]. The properties of the insulating material considered in this study were: ρc_p =100 $kJ/(m^3K)$, k =0.1 $W/(mK)$, with a coating layer thickness of 100 microns. These values were taken from the investigation of Kikusato et al. [2], who stated that an insulating material with these characteristics allowed reducing the heat losses through the walls of a Diesel engine.

To model the behavior of the 100 microns coating layer the solid was discretized with 1000 nodes in the 1D heat transfer program. In order to validate the accuracy of the results a mesh independence study was previously carried out. Fig. 5 shows that the mean temperature and mean heat flux values do not change significantly by increasing the number of cells above 500 already.

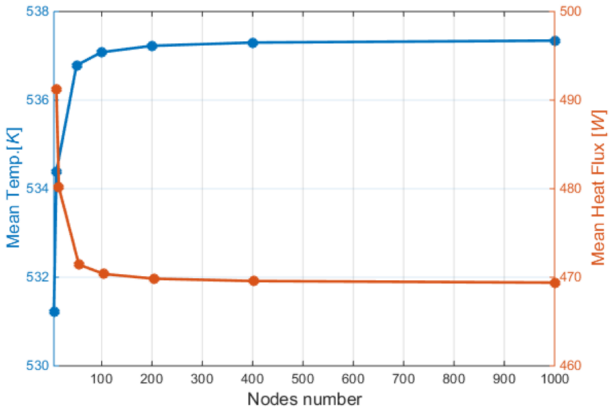

Figure 5: Mesh independence study

Fig. 6 shows the instantaneous temperature evolution during the full engine cycle of the gas exposed piston surface, as well as the gas temperature in the combustion chamber. The surface temperature follows a similar trend to that of the gas temperature trace and presents a high peak during the combustion phase. Clearly, the low values of the conductivity and heat capacitance allow reducing the heat transfer through the wall. Moreover, Fig. 7 presents the instantaneous evolution of the heat transfer coefficient and Fig. 8 the heat flux through the wall. The heat flux evolution and the wall temperature evolution are taken as references for the definition of the equivalent coating material with the multi-factorial test.

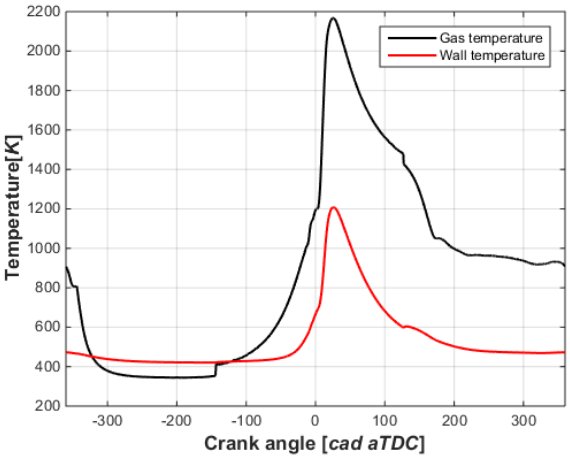

Figure 6: Instantaneous temperature evolution of gas and piston surface insulated with real thin coating during engine cycle

In particular, it is important that the 'equivalent material' with a greater thickness reproduces instantaneously the thermal evolution of the real thinner coating. For the equivalent coating a 2 mm thickness was considered, as it allows for a reasonable mesh size in CFD-CHT calculations. The multi-factorial DoE is performed within a range of values for heat capacitance and conductivity, in order to obtain the adequate physical properties of the equivalent material.

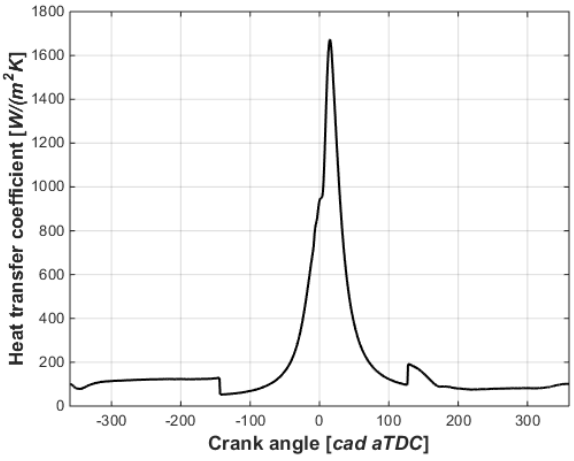

Figure 7: Heat transfer coefficient evolution during engine cycle for the real thin coating material

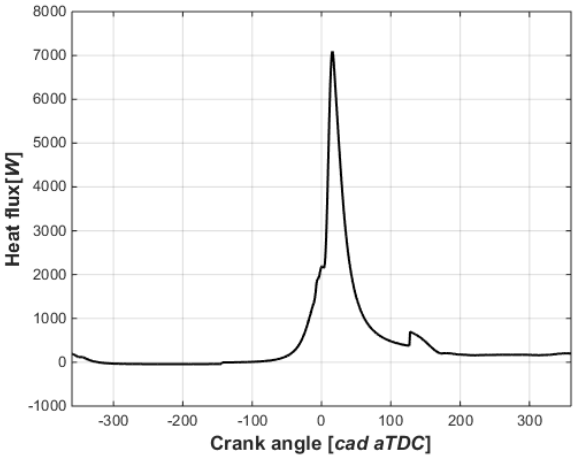

Figure 8: Heat flux evolution during engine cycle for the real thin coating material

First, a multifactorial test of possible combinations of heat capacitance and conductivity was carried out to find the instantaneous heat flux and temperature of each material.

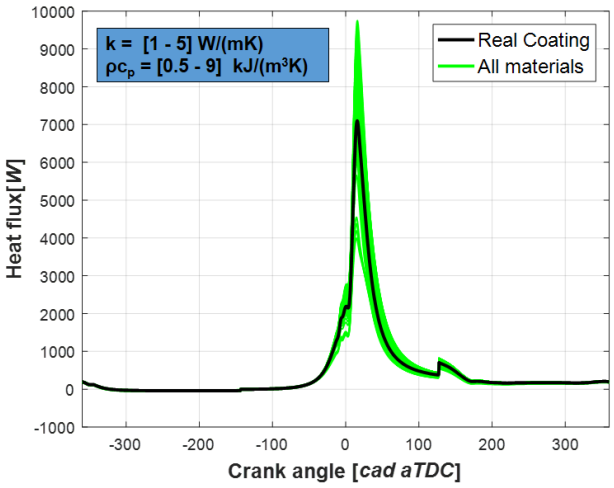

Figure 9: Heat flux temporal evolution for real coating and different equivalent materials

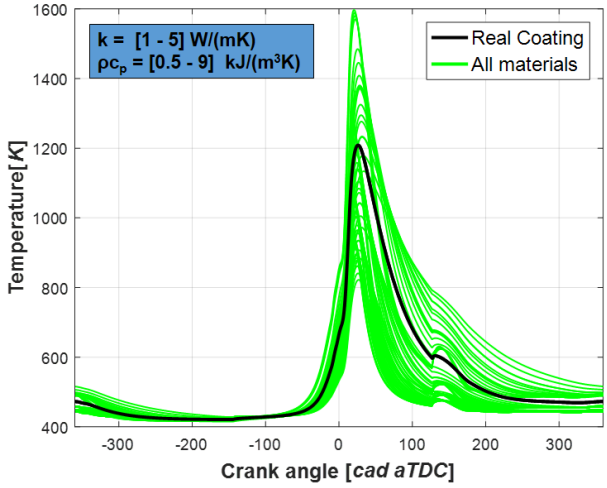

Figure 10: Wall surface temperature evolution for real coating and different equivalent materials

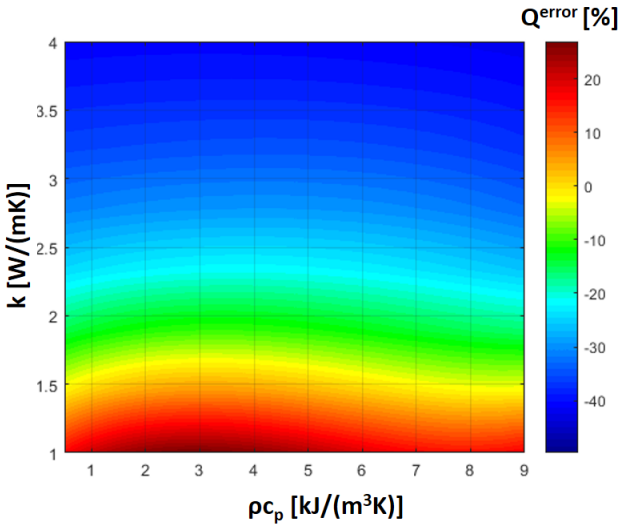

Figure 11: Determination of the possible combinations for the equivalent coating material

Figures 9 and 10 display respectively the heat flux evolution and wall temperature evolution obtained with the sweep of possible combinations of the material properties considered. As seen, it is quite difficult to find a solution whereby both the heat flux and the wall temperature traces match exactly the real coating material behavior. Since the coating is applied mainly to reduce the heat losses, the equivalent material should be primarily chosen to match the heat flux transient evolution. As shown in figure 6, the wall temperature is higher than the gas temperature during the intake stroke. Therefore, the heat flux is negative in this part of the engine cycle. The equivalent material should also reproduce this behavior. Hence, for selecting the best material, the errors for the positive, negative and mean heat fluxes have to be minimized in the equivalent material. Nonetheless, the temperature wall evolution was also taken into account in order to guarantee that it follows a very similar tendency to that of the real coating.

Since the possible combinations of the material properties are very large, a 2D least square fitting method was employed to find the optimal properties of heat capacitance and conductivity of the material. For this, we define the error Q^{error}:

$$Q^{error} = Q^{error}_{negative} + Q^{error}_{positive} \tag{14}$$

where $Q^{error}_{negative}$ and $Q^{error}_{positive}$ are the errors of the negative and positive heat fluxes, respectively. The target is to find the materials with $Q^{error} = 0$.

Then a sweep of the possible materials is performed by using a multiple lineal regression that best fits the DoE data. Fig. 11 shows the sweep of material coating properties obtained with the polynomial regression.

Finally, by applying a multiple regression analysis the optimal equivalent material is chosen as the one that minimizes the negative and positive heat flux errors. This is indicated as a black starred dot in Fig.12. This map also shows the sensitivity of the solution to the changes of the parameters. Note that a small change in ρc_p or k leads to discrepancies in the solution that are of the same order of magnitude as the possible gain in engine thermal efficiency obtained with this kind of coatings.($\backsim$ 3%).

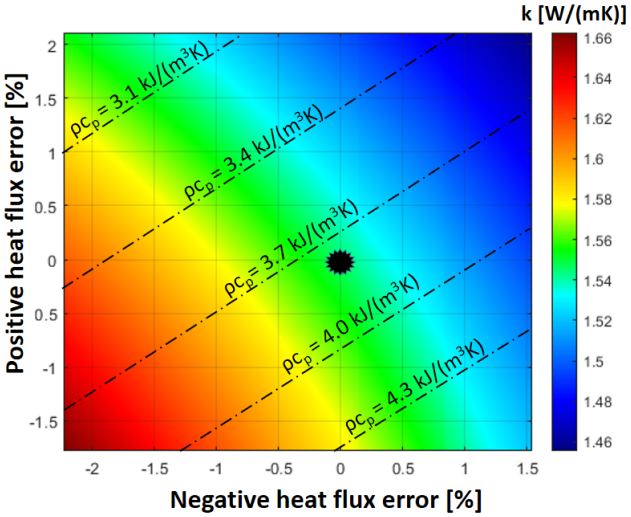

Figure 12: Analysis of the heat fluxes sensitivity to the equivalent material properties

4.2. Material selection

Fig. 13 shows the heat flux evolution of the newly defined equivalent material (ρc_p =3.769 $kJm^{-3}K^{-1}$, k =1.546 $Wm^{-1}K^{-1}$) compared with the real material. Although there are slight discrepancies, once quantified, the highest differences are for the mean flux with an error of -0.08%, while for the negative and positive fluxes the errors are -0.004% and 0.003%, respectively. This methodology based

on the adjustment of both ρc_p and k yields better results than the more classic resistance approach. The latter consists in treating the insulating layer as a heat resistance, thus neglecting its heat capacity. The results obtained with this approximation are also presented in Fig. 13. In this case, the errors are -16.8%, 10.1% and 10.2% for the negative, positive and mean heat fluxes, respectively. The details of the cases employed for the comparison are summarized in Table 1.

Table 1: Cases to evaluate the selected material

Case	Thick. $[mm]$	ρc_p $[\frac{kJ}{m^3K}]$	k $[\frac{W}{m \cdot K}]$
Real material	0.1	100	0.1
Selected material	2	3.769	1.546
Heat resistance	0.1	0	0.1

The results in terms of wall temperature evolution during the engine cycle, which are displayed in Fig. 14 confirm the above statement. The traces of the real and the equivalent coating materials show a very similar behavior, with a maximum discrepancy of 3% at peak temperature. This error is not really representative in terms of heat flux, so it is not significant. Nonetheless, it is important that the equivalent material should reproduce properly the thermo-swing of the real coating. Particularly when the exact wall temperature information is required, as is the case for instance to predict knocking in gasoline engines. For the case of the heat resistance, however, there is a maximum peak temperature difference with the real coating of 21%.

Finally, the chosen equivalent coating material can be applied to the engine walls in a 3D computational software where the heat transfer in all directions is taken into account.

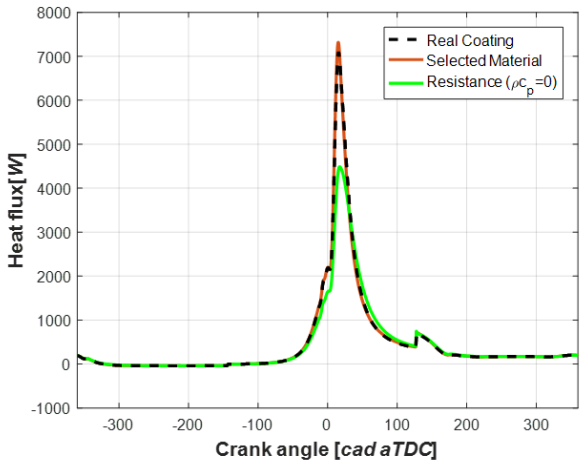

Figure 13: Heat flux evolution of the real coating, the selected equivalent material and a heat resistance

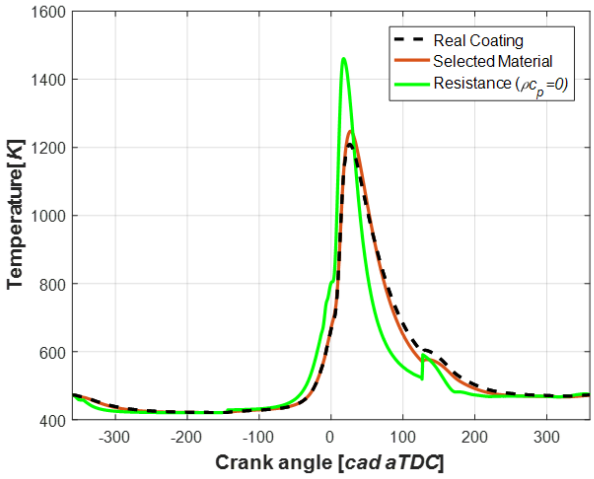

Figure 14: Surface temperature evolution for the real coating, the selected equivalent material and a heat resistance

4.3. Importance of number of mesh nodes and material thickness

As seen in the previous section, a multi-factorial test must be carried out in order to find a good equivalent material that behaves as the real coating. The multi-factorial sweep requires as input the thickness of the equivalent material. As explained in section 3.2, the thickness is chosen depending on the engine geometry, taking into account the minimum realistic cell size for the mesh. In the case of the engine shown in Fig. 4 a 2 mm coating layer was defined and meshed with 4 cells. This thickness is not added to the real engine geometry, as this would modify the compression ratio of the engine. Instead, the coated layer replaces an equivalent layer metal meshing. This has little influence on the heat transfer through the walls, since the heat transfer through metal is very low. It may be necessary to modify the equivalent material thickness and /or the number of nodes for the coating layer for meshing purposes when the geometry is complex. This could be the case for instance when applying coating on the cylinder head.

When the coated layer is meshed with different number of nodes the thermal behavior of the equivalent material changes. It does not reproduce anymore the behavior of the real insulating layer. It is also the case if the thickness considered is different. Hence in order to perform CHT calculations it is important to define the 'equivalent material' taking into account the effect of these parameters on the multi-factorial test solutions. The results of these parametric studies are described below. The reference solution is the one calculated above: 2 mm layer thickness and 4 nodes.

Figures 15 and 16 display respectively the heat flux and wall temperature evolution traces for the same material with a thickness of 2 mm changing the nodes number. In terms of heat flux, the traces are very similar, but the heat flux decreases as the number of nodes increases, especially

at peak flux. On the other hand increasing the number of nodes leads to higher temperatures on the wall surface, as expected, since the heat flux is proportional to the thermal gradient between the gas and the solid surface.

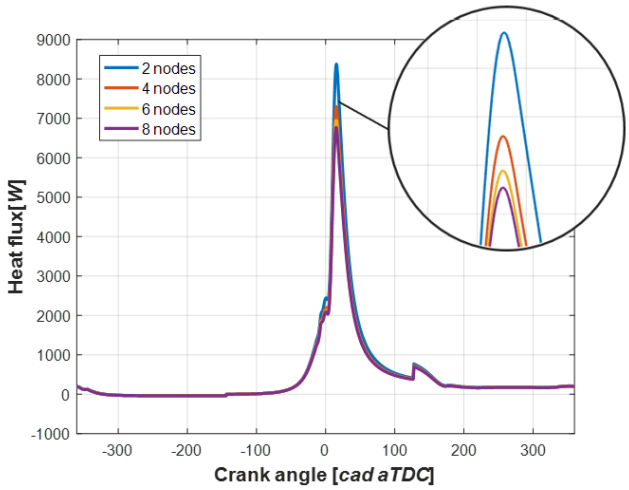

Figure 15: Heat flux evolution of the selected material for different number of mesh nodes

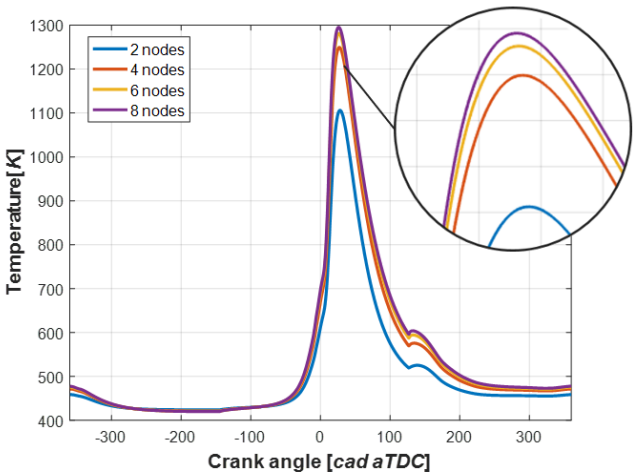

Figure 16: Wall temperature evolution of the selected material for different number of mesh nodes

The results of the multi-factorial tests performed by varying the thickness of the equivalent material are shown in figs. 17 and 18 in terms of heat flux temporal evolution and wall temperature evolution, respectively. The peak heat flux is not significantly affected by the thickness of the equivalent coating material. The traces start diverging after TDC, however, during the diffusion combustion process: there is less heat flux for increasing material thickness. The comparison of the wall temperature traces shows that these increase proportionally to the material thickness, though the peak temperature does not change significantly from 2 mm thickness onwards. This study clearly illustrates the necessity of properly defining the equivalent coating thickness before performing the CHT calculation.

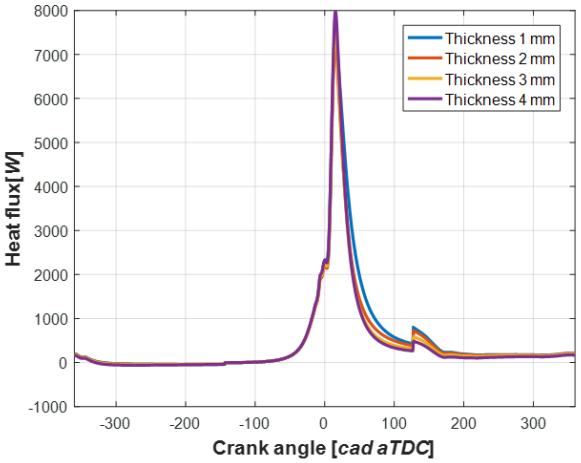

Figure 17: Heat flux evolution for different thicknesses of the selected equivalent coating material

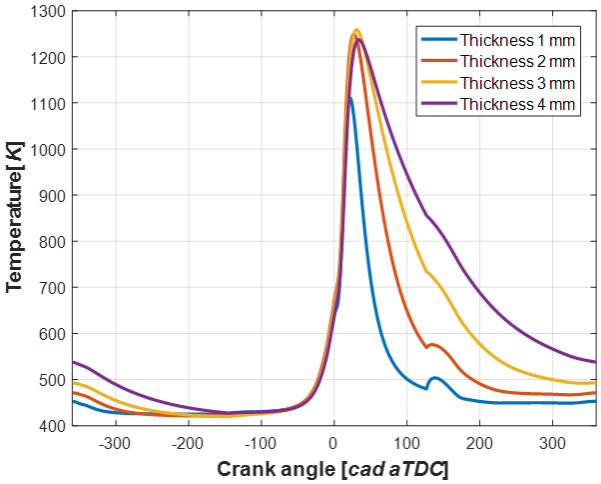

Figure 18: Wall temperature evolution for different thicknesses of the selected equivalent coating material

The material thermal properties calculated with the 1D HTM + multi-factorial model for different number of mesh nodes are given in Table 2 for an equivalent material thickness of 2 mm. The results show that the heat capacitance and thermal conductivity values increase as the number of nodes is higher. The same thermal properties obtained by varying the thickness are shown in Table 3 considering 4 nodes for the coating layer mesh. In this case, when the thickness grows the heat capacitance should be decreased and the thermal conductivity increased.

Table 2: Material properties for different number of nodes

Nodes	$\rho c_p\ [\frac{kJ}{m^3K}]$	$k\ [\frac{W}{m\cdot K}]$
2	2.774	1.047
4	3.769	1.546
6	4.132	1.703
8	4.328	1.780

Table 3: Material properties for different thicknesses of equivalent material

Thickness $[mm]$	$\rho c_p\ [\frac{kJ}{m^3K}]$	$k\ [\frac{W}{m\cdot K}]$
1	7.538	0.773
2	3.769	1.546
3	2.513	2.319
4	1.884	3.092

5. Conclusions

The 3D-CHT calculation of the heat transfer from the gas to the walls of a combustion chamber requires very fine meshing. Particularly so when the walls are coated with a very thin insulation layer (100 μm) as is the case for some recent studies performed to reduce the heat losses in engines. It is practically impossible to mesh such thin layers, as the computational cost becomes prohibitive. In this paper a methodology is presented whereby a 1D heat transfer model is used in combination with a multi-factorial test to define the thermal properties (conductivity and heat capacitance) of an equivalent coating material with reasonable thickness (e.g. 2 mm) that behaves as the real very thin coating layer. This equivalent material can then be adequately meshed to perform the CHT calculation and predict with accuracy the heat losses.

For a given reasonable coating thickness, various multi-factorial sweeps are necessary to identify the right combination of thermal properties of the new equivalent coating material. The selection criteria are primarily based on the comparison of the evolution during the engine full cycle of the positive, negative and mean heat fluxes of the real and equivalent materials. However, the wall surface temperature evolution during the engine cycle is also taken into account. The methodology has been demonstrated by calculating the equivalent material of a real coating defined by Kikusato et al [2]. Though the thermal properties of the equivalent material may not be realistic (meaning that this material does not physically exist), it does behave as the real coating material. In addition, a parametric study has been performed to study the effect of changing the number of meshing nodes and the thickness of the equivalent material on its thermal properties. This has demonstrated that it is important to adequately define the thickness and the number of nodes to mesh the equivalent coating material.

In conclusion, this approach is very useful for the 3D CHT simulation of the heat transfer through walls coated with very thin insulating layers, since it allows reducing very significantly the computational cost.

References

[1] P. Gori, C. Guattari, L. Evangelisti, F. Asdrubali, Design criteria for improving insulation effectiveness of multilayer walls, International Journal of Heat and Mass Transfer 103 (2016) 349 – 359. doi:https://doi.org/10.1016/j.ijheatmasstransfer.2016.07.077.

[2] A. Kikusato, K. Terahata, K. Jin, Y. Daisho, A numerical simulation study on improving the thermal efficiency of a spark ignited engine — part 2: Predicting instantaneous combustion chamber wall temperatures, heat losses and knock —, SAE International Journal of Engines 7 (1) (2014) 87–95. doi:https://doi.org/10.4271/2014-01-1066.

[3] W. Bryzik, R. Kamo, Tacom/cummins adiabatic engine program, SAE 1983 International Congress & Exhibition. doi:https://doi.org/10.4271/830314.

[4] G. Woschni, W. Spindler, K. Kolesa, Heat insulation of combustion chamber walls — a measure to decrease the fuel consumption of i.c. engines?, SAE 1987 International Congress & Exhibition. doi:https://doi.org/10.4271/870339.

[5] D. N. Assanis, E. Badillo, Transient heat conduction in low-heat-rejection engine combustion chambers, SAE 1987 International Congress & Exhibition. doi:https://doi.org/10.4271/870156.

[6] T. Hejwowski, Comparative study of thermal barrier coatings for internal combustion engine, Vacuum 85 (5) (2010) 610 – 616, the 7th International Symposium on Applied Plasma Science (ISAPS '09), Hamburg, Germany, 2009. doi:https://doi.org/10.1016/j.vacuum.2010.08.020.

[7] T. Li, J. A. Caton, T. J. Jacobs, Energy distributions in a diesel engine using low heat rejection (lhr) concepts, Energy Conversion and Management 130 (2016) 14 – 24. doi:https://doi.org/10.1016/j.enconman.2016.10.051.

[8] V. Garud, S. Bhoite, S. Patil, S. Ghadage, N. Gaikwad, D. Kute, G. Sivakumar, Performance and combustion characteristics of thermal barrier coated (ysz) low heat rejection diesel engine, Materials Today: Proceedings 4 (2, Part A) (2017) 188 – 194, 5th International Conference of Materials Processing and Characterization (ICMPC 2016). doi:https://doi.org/10.1016/j.matpr.2017.01.012.

[9] H. Kosaka, Y. Wakisaka, Y. Nomura, Y. Hotta, M. Koike, K. Nakakita, A. Kawaguchi, Concept of "temperature swing heat insulation" in combustion chamber walls, and appropriate thermo-physical properties for heat insulation coat, SAE International Journal of Engines 6 (1) (2013) 142–149. doi:https://doi.org/10.4271/2013-01-0274.

[10] G. Sivakumar, S. S. Kumar, Investigation on effect of yttria stabilized zirconia coated piston crown on performance and emission characteristics of a diesel engine, Alexandria Engineering Journal 53 (4) (2014) 787 – 794. doi:https://doi.org/10.1016/j.aej.2014.08.003.

[11] D. N. Assanis, T. Mathur, The effect of thin ceramic coatings on spark-ignition engine performance, in: Earthmoving Industry Conference Exposition 1990, SAE International. doi:https://doi.org/10.4271/900903.

[12] S. Shih, E. Itano, J. Xin, M. Kawamoto, Y. Maeda, Engine knock toughness improvement through water jacket optimization, Tech. rep., SAE Technical Paper (2003).

[13] P. N. Shrirao, A. N. Pawar, A. Borade, An overview on thermal barrier coating(tbc) materials and its effect on engine performance and emission, International Review of Mechanical Engineering 5 (5) (2011) 973–978.

[14] K. Osawa, R. Kamo, E. Valdmanis, Performance of thin thermal barrier coating on small aluminum block diesel engine, SAE 1991 International Congress & Exhibition. doi:https://doi.org/10.4271/910461.

[15] V. W. Wong, W. Bauer, R. Kamo, W. Bryzik, M. Reid, Assessment of thin thermal barrier coatings for i.c. engines, SAE 1995 International Congress & Exhibition. doi:https://doi.org/10.4271/950980.

[16] Y. Wakisaka, M. Inayoshi, K. Fukui, H. Kosaka, Y. Hotta, A. Kawaguchi, N. Takada, Reduction of heat loss and improvement of thermal efficiency by application of "temperature swing" insulation to direct-injection diesel engines, SAE International Journal of Engines 9 (3) (2016) 1449–1459. doi:https://doi.org/10.4271/2016-01-0661.

[17] A. Kawaguchi, H. Iguma, H. Yamashita, N. Takada, N. Nishikawa, C. Yamashita, Y. Wakisaka, K. Fukui, Thermo-swing wall insulation technology;-a novel heat loss reduction approach on engine combustion chamber, SAE Technical Paper 2016.

[18] P. Andruskiewicz, P. Najt, R. Durrett, S. Biesboer, T. Schaedler, R. Payri, Analysis of the effects of wall temperature swing on reciprocating internal combustion engine processes, International Journal of Engine Research 19 (4) (2018) 461–473. doi:https://doi.org/10.1177/1468087417717903.

[19] K. Fukui, Y. Wakisaka, K. Nishikawa, Y. Hattori, H. Kosaka, A. Kawaguchi, Development of instantaneous temperature measurement technique for combustion chamber surface and verification of temperature swing concept, SAE 2016 World Congress & Exhibition. doi:https://doi.org/10.4271/2016-01-0675.

[20] S. Caputo, F. Millo, G. Boccardo, A. Piano, G. Cifali, F. C. Pesce, Numerical and experimental investigation of a piston thermal barrier coating for an automotive diesel engine application, Applied Thermal Engineering 162 (2019) 114233.

[21] A. Headley, M. Hileman, A. Robbins, E. Piekos, P. Fleig, A. Martinez, C. Roberts, A thermal conductivity model for microporous insulations in gaseous environments, International Journal of Heat and Mass Transfer 135 (2019) 1278 – 1285. doi:https://doi.org/10.1016/j.ijheatmasstransfer.2019.02.073.

[22] P. Kundu, R. Scarcelli, S. Som, A. Ickes, Y. Wang, J. Kiedaisch, M. Rajkumar, Modeling heat loss through pistons and effect of thermal boundary coatings in diesel engine simulations using a conjugate heat transfer model, 2016, SAE Technical Paper.

[23] M. LEGUILLE, F. Ravet, J. Le Moine, E. Pomraning, K. Richards, P. K. Senecal, Coupled fluid-solid simulation for the prediction of gas-exposed surface temperature distribution in a si engine, Wcx^{TM} 17: Sae world congress experience, SAE International (mar 2017). doi:https://doi.org/10.4271/2017-01-0669.

[24] M. Wu, Y. Pei, J. Qin, X. Li, J. Zhou, Z. S. Zhan, Q.-y. Guo, B. Liu, T. G. Hu, Study on methods of coupling numerical simulation of conjugate heat transfer and in-cylinder combustion process in gdi engine (mar 2017). doi:https://doi.org/10.4271/2017-01-0576.

[25] L. Zhang, Parallel simulation of engine in-cylinder processes with conjugate heat transfer modeling, Applied Thermal Engineering 142 (2018) 232–240.

[26] A. Broatch, X. Margot, J. Garcia-Tiscar, J. Escalona, Validation and analysis of heat losses prediction using conjugate heat transfer simulation for an internal combustion engine, 14th international conference on engines vehicles, SAE International (2019).

[27] A. Broatch, P. Olmeda, X. Margot, J. Escalona, New approach to study the heat transfer in internal combustion engines by 3d modelling, International Journal of Thermal Sciences 138 (2019) 405 – 415. doi:https://doi.org/10.1016/j.ijthermalsci.2019.01.006.

[28] D. Hummel, S. Beer, A. Hornung, A conjugate heat transfer model for unconstrained melting of macroencapsulated phase change materials subjected to external convection, International Journal of Heat and Mass Transfer 149 (2020) 119205. doi:https://doi.org/10.1016/j.ijheatmasstransfer.2019.119205.

[29] A. Broatch, P. Olmeda, X. Margot, J. Gómez-Soriano, Numerical simulations for evaluating the impact of advanced insulation coatings on h2 additivated gasoline lean combustion in a turbocharged spark-ignited engine, Applied Thermal Engineering 148 (2019) 674 – 683. doi:https://doi.org/10.1016/j.applthermaleng.2018.11.106.

[30] P. Olmeda, V. Dolz, F. Arnau, M. Reyes-Belmonte, Determination of heat flows inside turbochargers by means of a one dimensional lumped model, Mathematical and computer modelling 57 (7-8) (2013) 1847–1852.

[31] A. Bejan, A. D. Kraus, Heat transfer handbook, Vol. 1, John Wiley & Sons, 2003.

[32] F. Payri, J. Luján, J. Martín, A. Abbad, Digital signal processing of in-cylinder pressure for combustion diagnosis of internal combustion engines, Mechanical Systems and Signal Processing 24 (6) (2010) 1767–1784.

[33] F. Payri, P. Olmeda, J. Martín, A. García, A complete 0d thermodynamic predictive model for direct injection diesel engines, Applied Energy 88 (12) (2011) 4632–4641.